J Mater Sci (2007) 42:1772–1781
DOI 10.1007/s10853-006-0986-7

Stability aspects of bulk nanostructured metals and composites

G. Wilde · H. Rösner

Received: 14 June 2006 / Accepted: 21 September 2006 / Published online: 12 December 2006

Abstract The requirement of thermal stability of nanocrystalline materials can be fulfilled with a composite approach. However, utilizing a two-phase approach includes additional constraints concerning the synthesis and processing, especially of massive nanostructured materials. Here, the potential of deformation processing for synthesizing nanoscale composite structures with uniform microstructures in bulk shape is analyzed for a series of Cu-rich alloys. The results are discussed with respect of governing materials properties that determine the feasibility of a composite approach in combination with severe plastic deformation to obtain massive nano-composite materials with high thermal stability.

Introduction

Nanostructured materials offer particular promise for new and potentially very useful products since they can have very different and often superior properties that crucially depend on the atomistic details of interior or exterior interfaces [1, 2]. As nanostructured materials are structures far away from thermodynamic equilibrium and since they have short transport pathways given by the grain boundaries [3], fast diffusion and rapid transformation kinetics often lead to coarsening and to the deterioration of the microstructure and the associated properties. Thus, ensuring the stability of the nanoscale structures, e.g., by utilizing a composite approach, is a key issue. This approach, however, imposes additional constraints on processing-related issues as well as on the stability of phases and phase mixtures and on phase transformations within the nanoscale structural units due to size confinement [4–6] and due to the presence of internal heterophase interfaces [7]. While some basic issues concerning the stability and concerning phase transformations of nanostructured composites have been identified and discussed recently [8], processing-related issues still require focused attention if a transition from laboratory-scale—to application-relevant quantities is envisaged. One way for processing larger quantities of material to obtain massive nanocrystalline specimens (a nanocrystalline specimen is regarded as ''massive'' if the length in all spatial directions exceeds the grain size by at least a factor of 1,000) the characteristic size of the building block, i.e., the grains, is given by deformation processing at room temperature [9–11]. In this respect, repeated cold-rolling with intermediate folding, which will be described as ''cold rolling'' in the following, has been shown to be capable of producing the smallest grain size obtained so far via deformation processing of polycrystalline material with initial grain sizes in the micrometer range [12]. Particularly promising with respect to adjusting optimized microstructures, e.g., grain refinement and green density, while allowing also for massive pieces to be processed are new options given by the sequential combination of different non-equilibrium processing pathways that

G. Wilde (✉)
Institute of Materials Physics, University of Münster,
Wilhelm-Klemm-Str. 10, Muenster 48149, Germany
e-mail: gwilde@uni-muenster.de

H. Rösner
Institute of Nanotechnology, Forschungszentrum Karlsruhe,
76021 Karlsruhe, Germany

drive a material to a different extent-, with different rates—and by different means from thermodynamic equilibrium [13]. In addition to synthesis pathways that are solely based on plastic deformation, vitreous quenching products can provide additional access to nanostructured composite formation by thermally induced nanocrystal formation [14], or—as recently demonstrated for marginally glass forming, Al-rich alloys that show the formation of extremely large number densities of uniformly sized nanocrystals—via severe plastic deformation by high-pressure torsion straining (HPT) [15]. Detailed analyses have indicated that the nanocrystals form mostly in shear bands but continued deformation also leads to fragmentation of the existing nanocrystals if their size exceeds a critical limit [16]. The two counteracting processes, i.e., growth and fragmentation, apparently lead to a steady-state crystal size, resulting in a uniform dispersion of nanocrystals of similar sizes within a residual amorphous matrix. The synthesis routes towards massive nanocrystalline metals and composites as well as two additional examples that utilize a fully or partially liquid route are summarized in Fig. 1 together with current examples of the respective microstructure types.

Options for synthesizing nanocrystalline dual phase materials are attractive in more than one way and in addition to the stabilization effect: with multicomponent and—more importantly—multiphase materials, the most important tool of modern materials design would also become accessible for adjusting the often advanced or new properties of nanocrystalline materials to yield even more enhanced performance or functionality. Thus, it is important to analyze possible processing pathways such as severe deformation that allow synthesizing nanostructured multiphase materials with a uniform microstructure from a coarse-grained starting state. Co-deformation of two components that are mutually immiscible also bears the potential to yield nanostructured composites. Depending on the relative amounts of both components and on their propensity for forming and retaining nanoscale (micro)structures, either a nanostructured phase embedded in a polycrystalline matrix or composites consisting of two nanostructured phases should be obtainable. In this respect, amorphization [18] and the formation of metastable or even unstable solid solution phases [19] are competing processes that may prevent the synthesis of completely nanocrystalline two-phase composites. Here, experimental results on nano-composite formation of binary systems with different heats of mixing are summarized and discussed. In addition, a short excursion on the thermal stability of single-phase nanostructured materials and its relation to processing history is included for comparison.

Experimental procedures

Repeated cold-rolling with intermediate folding (F&R) of sheet or ribbon material has been applied as one optional technique for applying very high strains at moderate strain rates of the order of less than 0.5 s^{-1} [20–22]. In contrast to the deformation processes that are conventionally summarized as SPD processes [9, 10], cold rolling proceeds without the simultaneous application of a high hydrostatic pressure. In fact, the hydrostatic component of the pressure during rolling with the geometry of the rolls used here is always less than 0.8 GPa [11]. The procedure has been described in detail elsewhere [11, 23]. In principle, an initial stack of thin foils is deformed by rolling at decreasing roll gap and folded after reaching a minimum thickness of about 100 μm. At this point, the sample is cut or broken in half, stacked and the procedure is started again. The entire process between two consecutive folding operations is denoted in the following as one rolling pass. The deformation time and the respective strain rate were calculated from the geometry of the rolls (diameter of the rolls 150 mm, length of the rolls 100 mm), the circumferential roll velocity (1 m/min) and the thickness of the samples (200–300 μm). In fact, the actual strain rate is smaller than the calculated upper bound, because of sliding at the internal interfaces (due to imperfect bonding) and due to certain areas of the sample that do not overlap after the folding. Consequently, a small area fraction is not deformed during rolling, as also described by Bordeaux et al. [21]. Moreover, the bending of the rolls that inevitably occurs is not included in the simplified calculation. Thus, assuming plain strain conditions leads to an overestimation of the amount of strain, which is the physical parameter that drives the microstructure modification. Due to these differences between the actual strain and the calculated theoretical value, the strain state will be denoted by the number of folding and rolling passes rather than by the corresponding theoretical value of the equivalent strain. Approximately, the maximum number of F&R cycles (100 times) corresponds to an equivalent strain of $\varepsilon = 80$!

Specimens for cold-rolling were cut from initial foils (area: 20 mm by 20 mm) and stacked in the right proportion to yield the desired nominal composition. The initial stack consisted of at least 10 stacked pieces. The initial thicknesses of the elemental foils and the purity levels were as follows: Ag: 25 μm, 99.998%, Co:

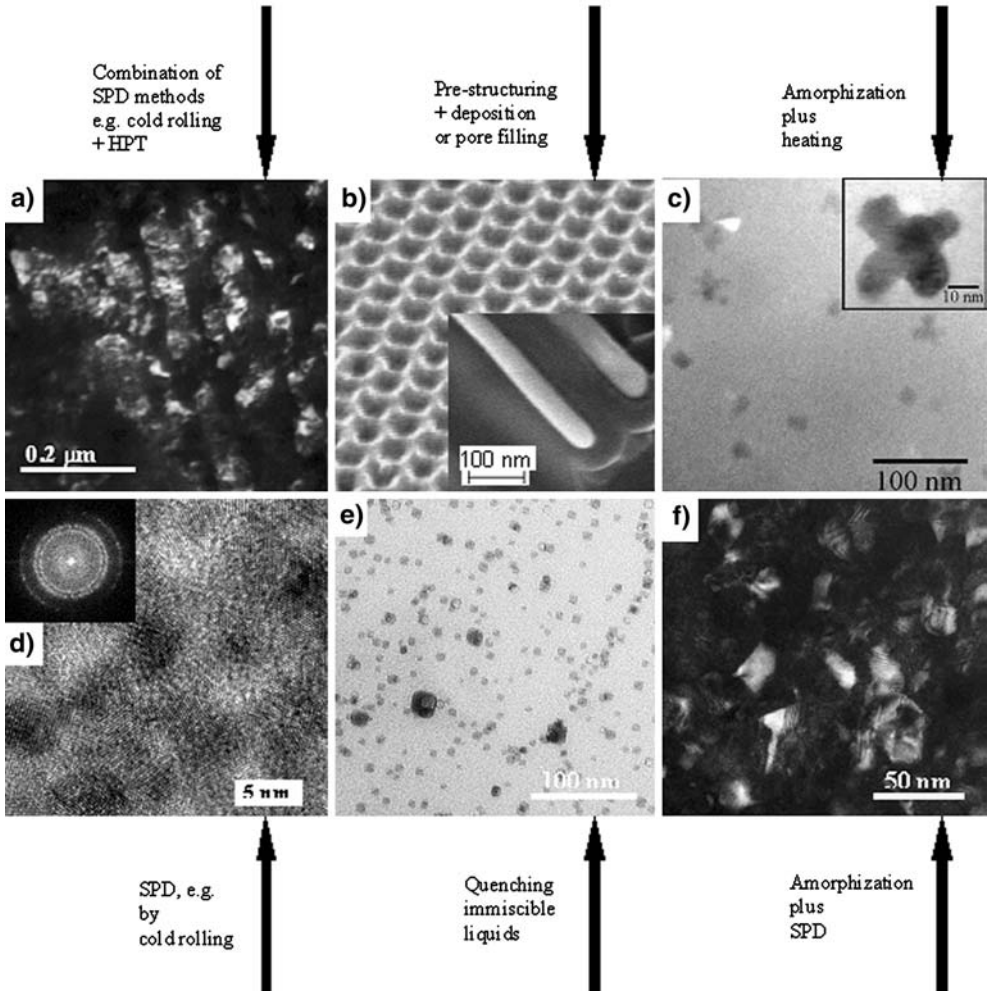

Fig. 1 Examples of nano-composite microstructures that have been realized by different synthesis pathways. (**a**) Dark-field TEM micrograph of pure Pd after repeated rolling and folding and subsequent high pressure torsion straining. (**b**) Nanoporous Alumina membrane prepared by anodic oxidation of Al sheet (as described e.g., in [8]). The inset shows the same template after pressure-assisted pore filling with a low-melting eutectic (Bi–Cd). (**c**) Al nanocrystals within an amorphous Al-rich matrix. The base alloy ($Al_{88}Y_7Fe_5$) is a marginally glass-forming material that shows the occurrence of the so-called nanocrystallization [14]. (**d**) High resolution TEM micrograph of pure Ni after repeated rolling and folding. (**e**) Immiscible $Al_{99}Pb_1$ alloy that has been obtained through rapid melt quenching by melt spinning. The nanocrystalline microstructure of Pb is sufficiently stable to remain at very small crystallite size even after repeated melting [5, 17]. (**f**) $Al_{88}Y_7Fe_5$ after initial amorphization by rapid quenching and after subsequent severe plastic deformation of the amorphous quenching product by high-pressure torsion straining [15]

100 μm, 99.995%, Cu: 25 μm, 99.999%, Ni: 100 μm, 99.994%, Zr: 25 μm, 99.9+%.

The samples were investigated by X-ray diffraction (XRD, Phillips X'Pert) in Bragg-Brentano geometry with Cu-K_α radiation using a fast, position-sensitive detector (Phillips X'Cellerator). Afterwards, the characterization of their morphology was performed in cross section by scanning electron microscopy (SEM, Leo 1530). For transmission electron microscopy/selected area electron diffraction investigations (TEM/SAED, Philips Tecnai F20 ST), 3 mm in diameter plan view samples were mechanically punched out. Additionally, small pieces with dimensions less than 3 mm were glued into a hollow cylinder and then cut into thin discs for cross-section transmission electron microscopy preparation. Thereafter, the samples were either thinned by twin-jet electropolishing (1/3 nitric acid and 2/3 methanol), as e.g., pure Ni, or samples were thinned by ion milling with a low accelerating voltage (3.5 kV) to minimize the beam effects on the microstructure. The heat evolution during continuous heating experiments was monitored by differential scanning calorimetry with a power-compensating device (DSC, Perkin Elmer Pyris 1).

Two-phase nanocomposites by severe plastic deformation

One promising way to address two general issues: the synthesis of bulk quantities and the synthesis of material with uniform microstructures is given by repeated rolling and folding at room temperature. In contrast to non-equilibrium processing methods that are based on rapid heat release, deformation processing by repeated folding and rolling proceeds essentially at room temperature. Thus, the metastable extensions of the phase equilibria and even possible non-equilibrium states that are sampled during the synthesis are potentially extended for the deformation-based synthesis route [24]. Therefore, several binary Cu-rich alloys have been studied that contain alloy constituents with rather different heat of mixing values with Cu. Specifically, alloys of the binary systems Cu–Co, Cu–Ag, Cu–Ni and Cu–Zr were processed by repeated folding and rolling. With these alloy systems, their heat of mixing varies from strongly positive values for Cu–Co to almost zero (Cu–Ni) and to strongly negative values (Cu–Zr).

Cu–Zr

As expected from general considerations concerning the minimization of the free enthalpy, the alloy with strong negative heat of mixing shows an amorphization reaction of a considerable volume fraction after initial grain size reduction into the range of ultrafine grained structures, i.e., with $d < 100$ nm. After 40 F&R passes, a broad diffuse maximum in the X-ray diffraction spectrum, characteristic of an amorphous phase and centred at about $2\theta = 40^{o}$ appeared along with some weak crystalline diffraction peaks due to residual pure Cu and Zr. This result is in agreement with earlier findings [20]. Doubling the F&R passes leads to a fully X-ray-amorphous sample without any indication of a residual crystalline fraction. The continuous increase of strain during repeated cold rolling and folding of the multilayer sample resulted in a decrease of the average layer thickness with continuously increasing total interface area. The average elemental layer thickness and amorphous layer thickness estimated from scanning electron microscopy, dark-field transmission electron microscopy and high-resolution transmission electron microscopy micrographs [12] is shown in Fig. 2. In the early stage, cold rolling leads to a fast decrease of the layer thickness. Further refinement occurs slowly after severe deformation. The average layer thickness is about 1 μm after 10 F&R cycles and 15 nm after 20 F&R cycles. Further processing up to 40

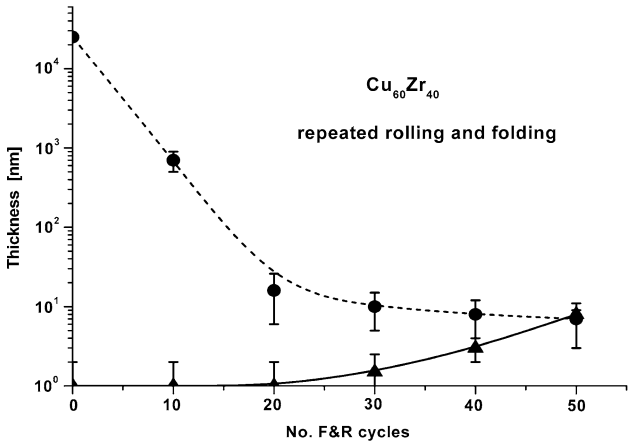

Fig. 2 Change in elemental layer thickness (●) and amorphous layer thickness (▲) of $Cu_{60}Zr_{40}$ as a function of the number of rolling and folding passes

F&R cycles results in a refinement of the individual layers thickness that varies between 7 nm and 10 nm. No layer structure was observed after 50 F&R cycles because the samples reach an almost completely amorphous state at that deformation level. In addition to the layer thickness, the grain shape has also been studied as a function of total strain. In principle, the grain shape first becomes elongated in the layer plane during the early stages of rolling and folding. After several passes, when the layer thickness becomes small, the ''pancake''-shaped grains become equiaxed, as observed by plane-view and cross-section TEM analyses. The transformation from elongated to equiaxed grains is most probably due to the accumulation of dislocations during continued deformation that form new high-angle grain boundaries via dislocation pile-up and subgrain formation [12]. Similar behavior has been observed for several pure metals and binary alloys, indicating that the observed microstructure development is characteristic for the rolling and folding process. These results, as well as similar results obtained on different binary, ternary and quaternary alloys with strongly negative heat of mixing indicate that completely nanocrystalline composites cannot be obtained directly by deformation processing of alloys with a highly negative heat of mixing. In such cases, an additional heat treatment of the amorphous phase might induce the formation of a nanocrystalline microstructure if the thermodynamic and kinetic conditions are in favor of copious crystal formation [25].

Cu–Ni

With Cu–Ni, the thermodynamics of the system can be approximated reasonably well by a regular solution

model, i.e., with a constant heat of mixing that does not depend on composition. Thus, forced mixing due to shear and due to friction at the interfaces as well as the reduction of the free enthalpy due to a reduction of interfaces upon alloy formation should lead to early mixing, that is the formation of solid solutions at small numbers of rolling passes. The XRD spectra taken on $Cu_{60}Ni_{40}$ samples after different numbers of rolling passes shown as Fig. 3 confirm this expectation. The data clearly show a shift of the lattice parameters of the two constituents with a more pronounced shift for the Cu-rich solid solution, as to be expected since it is known that Ni diffuses extremely rapidly into Cu while Cu shows conventional diffusion behaviour in Ni [26]. After 70 rolling passes, the spectra of the two fcc-solid solutions have completely merged, indicating complete alloying at room temperature and the formation of an extended solid solution. TEM analyses indicate the formation of an ultrafine-grained microstructure at this deformation stage (Fig. 4a). Upon continued deformation by rolling and folding, the average grain size reaches a steady state value of 80 ± 40 nm. Compared to the minimum grain sizes obtained for the pure elements Cu and Ni by repeated rolling and folding at room temperature, i.e., d_{min} = 8 nm for Ni [11, 12] and d_{min} = 140 nm for Cu [27], the results concerning the grain size reduction of the Cu–Ni alloy suggests that the steady-state grain size scales with the alloy composition. This result confirms that true alloying has occurred at room temperature since the steady state grain size of a regular solution system should scale with the respective melting temperature. Moreover, the result also indicates that the steady state grain size is controlled by the atomic mobility that, in turn, scales in a first order approximation with the melting temperature. Obviously, the thermal stability of the fine-grained microstructure is also determined by the atomic mobility. In principle, the steady state grain size is thus determined by a dynamic equilibrium between defect generation and defect annihilation. It has been observed that even minor alloying additions, especially those that have a strongly negative segregation enthalpy, result in a stabilization of microstructures at rather small grain sizes [28]. Yet, alloying additions with a completely miscible component should not effectively stabilize fine-grained microstructures. Thus, achieving smaller grain sizes via deformation processing for any given material requires either that the deformation proceeds at a lower temperature so that the annihilation rate is decreased, or that the rate for defect generation is increased at constant annihilation rate.

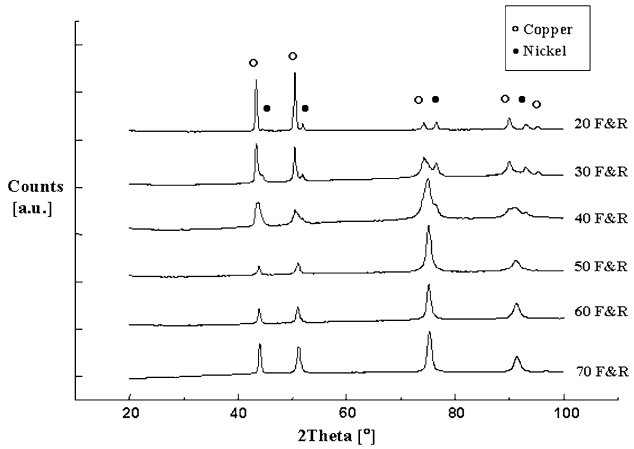

Fig. 3 XRD theta—2 theta scans of as rolled $Cu_{60}Ni_{40}$ samples after different numbers of rolling and folding passes. The elemental peaks of Cu and Ni disappear during the deformation. After 50 rolling passes, the sample appears to be completely intermixed

However, heating the material after 70 F&R passes to 560 °C does not result in forming a coarse-grained polycrystalline microstructure with micron-sized grains. Instead, the grain size stays within the ''ultra-fine'' size range, i.e., it remains at about d = 200 ± 40 nm (Fig. 4b). This result is astonishing, since the annealing temperature is higher than half the thermodynamic melting temperature, i.e., in a temperature range where usually massive coarsening occurs. Thus, it seems that the alloying effect is capable to allow for an increased stability of ultrafine-grained structures, even for alloy systems where nanocrystalline microstructures are not obtained. In this respect, small compositional heterogeneities will occur necessarily during the co-diffusion of two species with different diffusivities, which result in the formation of localized and transient concentration gradients. Such gradients slow down the local diffusion, leading to an effective grain size stabilization since a non-uniform interface movement would produce additional interface coupled to an increase in free energy, which is not favorable.

Cu–Ag

In terms of the well-known Hume-Rothery rules, the eutectic Cu-Ag system is peculiar as the two noble fcc metals, with atomic size difference still within the 15% limit, are almost completely immiscible below ~650 K [29]. The system shows a positive heat of mixing (positive ΔH) in the solid as well as in the liquid state [30]. While the atomic size mismatch of about 13% must have contributed to the low solid solubility, this size factor is apparently not sufficient to favor easy

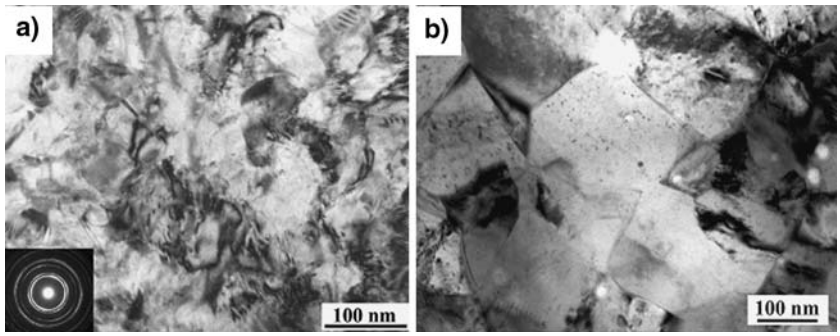

Fig. 4 Bright-field TEM micrographs of $Cu_{60}Ni_{40}$ after 70 rolling and folding passes, (**a**) directly after the deformation and (**b**) after an additional heating treatment (20 K/min, up to 560 °C) in the DSC

amorphization in this system. In fact, the vast majority of the alloys produced so far are fcc crystalline solid solutions, even when at the eutectic composition. Here, it is of interest to compare the grain-size reduction behavior as well as the thermal stability of the fine-grained material for an alloy with small positive heat of mixing.

Figure 5 displays the XRD patterns of the cold rolled foils after different passes. After rolling, the main diffraction peaks (the peaks for (111) near 40° in 2θ) shift and merge into each other, indicating that alloying occurred. It is interesting to note that the intensity of the first peak is much weaker, and its width is much wider, than those of the XRD peaks of fcc solutions formed by deposition or ball milling (typical full width at half maximum less than 2° in 2θ [31–34]. Overlapping broad peaks from residual elements and/or strong compositional non-uniformity in the rolled samples would contribute to the halo-like feature. However, this peak did not sharpen after a large number of passes. Another possible contributing factor is the existence of a broad halo from amorphous fractions. TEM examination indeed indicate the presence of local amorphous regions in repeatedly cold-rolled Cu–Ag samples, as shown in the high-resolution image of Fig. 6 that displays an area with predominantly amorphous features that are obviously different from the lattice fringes of neighboring residual crystals (in the middle of the upper section of the image). There is also an apparent halo in the SAED pattern, Fig. 6, in addition to spots/rings from the crystals. Heating the as-rolled alloy in the DSC to different temperatures results in decomposition into Ag-rich and Cu-rich phases as indicated in the XRD-spectra that were taken after the heating treatments (Fig. 7). At 260 °C, nano-grained Ag and Cu terminal phases are clearly dominant in the sample volume.

These results indicate on one hand that under conditions that are far from thermodynamic equilibrium, as sampled for example during severe plastic deformation treatments and under the additional boundary condition of ultra-fine—or even nanocrystalline grain sizes, even for alloys with a positive heat of mixing, solid solution formation and (partial) amorphization can occur. These results emphasize the findings

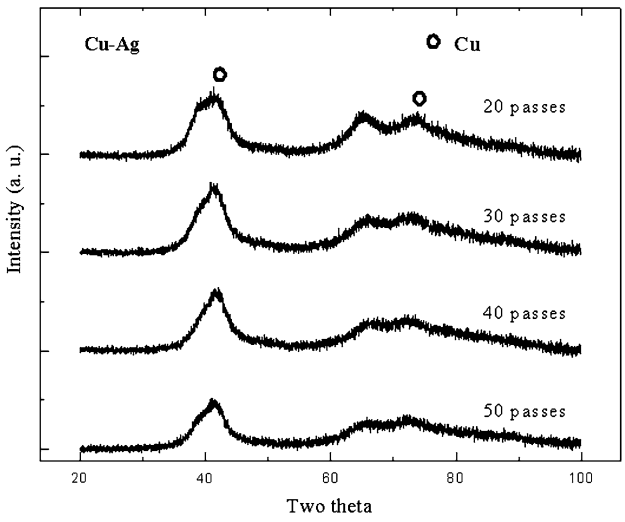

Fig. 5 XRD patterns of cold rolled $Cu_{60}Ag_{40}$ after different numbers of rolling and folding passes

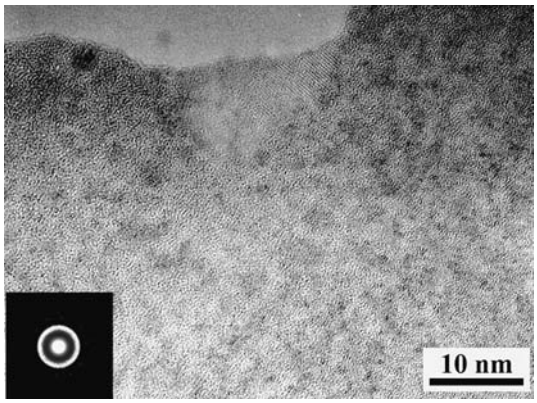

Fig. 6 High resolution TEM micrograph of cold rolled $Cu_{60}Ag_{40}$ (70 folding and rolling passes), together with selected area electron diffraction patterns

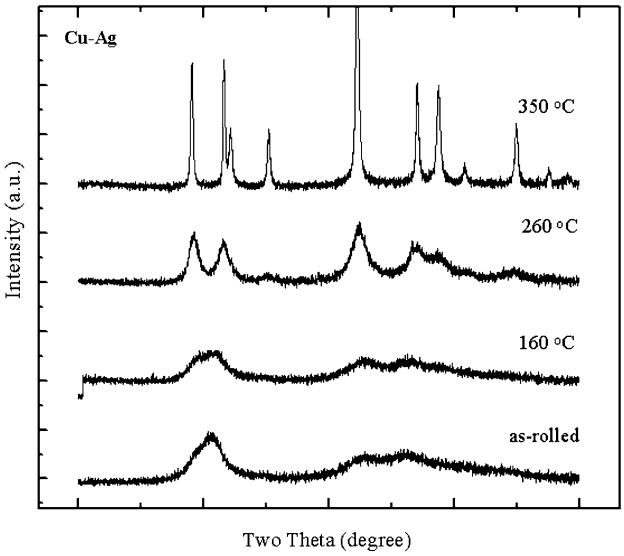

Fig. 7 XRD patterns of cold rolled $Cu_{60}Ag_{40}$ after DSC-heating measurements to different temperatures. Prior to heating, the samples were cold-rolled and folded for 70 times

concerning changes of the phase stability at small system size that are also—at least partially—thermodynamic in nature [7, 17]. Moreover, the response upon heating the fine-grained/amorphous Cu–Ag mixture indicates an unusually high thermal stability, e.g., compared with pure nanocrystalline Cu that coarsens even at room temperature [35], and a decomposition/crystallization into a nanocrystalline composite as opposite to the formation of a polycrystalline microstructure with coarse grains, although the heat treatment has been performed at a high homologous temperature, i.e., at a temperature that was more than half the value of the eutectic temperature! In fact, a similar stabilization strategy that is based on the immiscibility of two phases has also been shown to hold up to high temperatures for nanostructured oxide systems [36].

Cu–Co

The Cu–Co system has been chosen as an alloy system with large positive heat of mixing, as also indicated by the presence of an extended metastable miscibility gap in the undercooled liquid state of the alloy [37]. Upon repeated cold rolling starting from elemental foils in a multilayer sandwich, the layer thickness is reduced by homogenous deformation and additionally due to pronounced multiple necking [21] that occurs as a result of the large difference of the shear modulus values. Within the necking regions that present regions of high stress concentration, non-equilibrium mixing can occur [21, 24]. However, the thermodynamics of the system prevent amorphization to occur, so that the metastable solid solution cannot reach the kinetically arrested state of the glass. In fact, the microstructure observed by TEM after 70 F&R passes consist of a fine-grained nanostructure with high defect densities (Fig. 8a). When a partial or even a complete solid solution is obtained for a system with a high positive heat of mixing, then upon heating the occurrence of decomposition is highly likely. In fact, this transformation

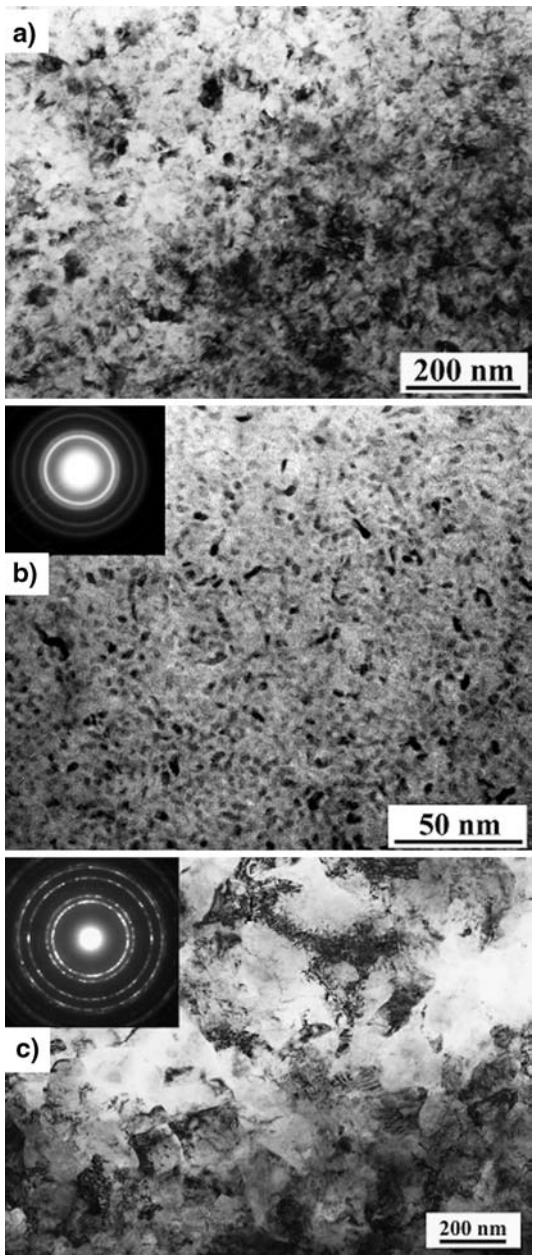

Fig. 8 Bright-field TEM images of: (**a**) $Cu_{60}Co_{40}$ 70 times cold rolled and folded. (**b**) $Cu_{60}Co_{40}$ 70 times cold rolled and folded and annealed at 250 °C for 4 h. (**c**) The same material but annealed at 560 °C for 30 min

should precede any coarsening or grain growth, since the microstructure that is received after processing is not stable and thus cannot grow. Therefore, metastable solid solutions of immiscible alloys can be expected to show a tendency for developing a smaller grain size upon heating to moderate temperatures.

Such a tendency is quite unusual since conventionally, materials coarsen more rapidly at increased temperatures. Yet, in cases where metastable solution formation is obtained at a given grain size d_0, the free enthalpy, G, with: $G = G_0 + \delta G$ with $G_0 = H$–TS and δG summarizing the thermodynamic excess due to the supersaturation and due to interfaces and defects, might develop a local minimum at a grain size d with the possibility for $d < d_0$. A requirement for this scenario is a negligible long-range diffusion, which is approximately fulfilled for systems with low miscibility. With

$$\delta\, G = \sum_i A_i \times\ \sigma_{\,i} \ +\ \psi\ +\ \Delta\, H_{\mathrm{mix}} \qquad (1)$$

A_i is the total interface area of all interfaces of the i-type that have the specific interface free energy σ_i. ψ summarizes the defect contributions due to dislocations (that scale with the square of the respective burgers vectors), microstrain or non-equilibrium vacancies. ΔH_{mix} represent the mixing enthalpy that is released if the metastable solid solution decomposes into the equilibrium phases. Here, we assume that the composition of the sample is homogeneous before the heat treatment. Due to the constraints concerning long-range diffusion, the material cannot easily gain ΔH_{mix} by diffusional rearrangement but needs to form regions of the equilibrium compositions with new interfaces separating Co-rich and Cu-rich grains. Thus, as a first step towards equilibrium, thermally induced grain refinement via phase separation and precipitation should occur!

The extent to which such a grain refinement can occur is controlled by the counteracting contributions from the interface free energy (that favors large grain sizes even at supersaturation) and from the mixing enthalpy (that favors phase separation for $\Delta H_{\mathrm{mix}} > 0$) and their relative magnitude. As long as rapid diffusion is prevented, which is the case after low-temperature annealing that decreases the defect density, and with the additional stabilization at small grain size due to the higher solubility in the grain boundary volumes, the kinetic stabilization of small grain sizes in the range of few tens of nanometers might be effective even at rather elevated temperatures. In order to perform an initial test of the above-described scheme, the severely deformed Cu–Co alloy has been heat-treated. After annealing at low homologous temperature (i.e., at 250 °C for 4 h), clearly separated phases that are Co-rich or Cu-rich, respectively, are observed (Fig. 8b). Remarkably, the grain size after the annealing treatment is much smaller than the grain size observed directly after the rolling and folding deformation. In fact, this experimental result confirms our suggestion concerning the possibility for a thermally induced grain size reduction. Similar results have been obtained for a $Cu_{60}Fe_{40}$ alloy. If the material is heated to higher temperatures, coarsening sets in due to the diffusional rearrangements that can occur at elevated temperatures and that are driven by the minimization of the total free enthalpy via coarsening and grain growth. However, even after annealing at 560 °C for 30 min, the microstructure remains in the range of ultrafine-grained materials with an average grain diameter of only 110 nm (Fig. 8c). This small grain size again demonstrates the feasibility of the stabilization strategy that is based on immiscible alloying additions.

Pure nanocrystalline metals

In contrast to applying a two-phase approach where stabilization is based on kinetic and thermodynamic reasons associated with multicomponent alloy design as described above, mono-elemental nanostructured materials are very often described by two-phase models with a ''grain boundary-'' and a ''core phase'' [38]. Recent investigations of deformation-induced grain refinement leading to ultra-fine grained or even nanocrystalline microstructures and reports that show unequivocal evidence for strain-induced coarsening of material with nanometer-sized grains [39] as well as the observation of rather dissimilar thermal stabilities of nanocrystalline material of identical grain size but different synthesis pathway suggest that the processing dependence of the grain boundary structure needs to be taken into account when the thermal stability of a nanostructured material is analyzed. Yet, the experimental observations are far from being a result of systematic studies and so far most of the aspects remain poorly understood. In particular, two observations are revealing: (A) Nanocrystalline material when synthesized via gas-phase processing and compaction coarsens during plastic deformation even if the deformation proceeds at low strain rate, low pressure and at ambient temperature. (B) Nanocrystalline material that was synthesized by severe deformation (i.e., rolling and folding) exhibits enhanced thermal stability compared to material of similar grain size that has been produced by gas-phase condensation and that shows

considerable coarsening on a time scale of days even at room temperature.

The rather high thermal stability of material synthesized via plastic deformation is indicated in Fig. 9 that shows a comparison between pure Ni that was rolled and folded at room temperature for 80 times [11] (Fig. 9a), and the same material after additional high-pressure torsion straining (HPT) [13] (5 turns under 6 GPa at 100 °C) and annealing for 30 min at 300 °C (Fig. 9b). Clearly, the average grain diameter after the annealing treatment is still considerably below 100 nm! It should be noted that the grain size after HPT processing was already increased to about 35 nm. A Ni sample that was subjected to the identical heat treatment directly after rolling and folding showed a larger grain size of about 130 nm. Thus, from the two samples with identical chemical composition and with partly identical processing history, the one with the larger defect density (particularly with higher dislocation density) shows a higher thermal stability. Estimates obtained form high resolution transmission electron microscopy images, such as published in [13], yield dislocation density values of about 5×10^{15} m^{-2} and higher for the material after rolling and folding and HPT. A similar observation was made for Pd, where samples were obtained from inert gas condensation, from cold rolling and from cold rolling plus HPT. Also with these samples, the material with the lowest density of dislocations (the material synthesized by inert gas condensation) showed the lowest thermal stability.

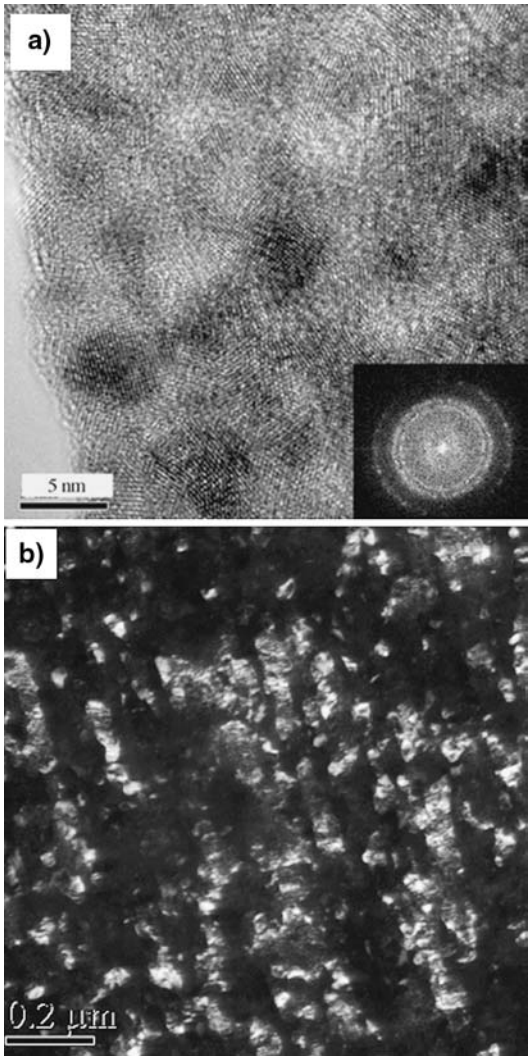

Fig. 9 (**a**) HR-TEM micrograph of Ni that has been rolled for 80 passes ($\varepsilon = -56$). The inset at the bottom right corner shows the FFT-pattern. (**b**) Dark-Field micrograph: overview showing the microstructure of HPT-Ni after annealing at 300 °C

Interestingly, investigations concerning the impurity level including carrier gas - hot extraction in inert gas atmosphere have revealed that the nanocrystalline samples that have been produced by such largely different synthesis pathways include almost identical impurity levels, especially with respect to O_2, N_2 and H_2. This result eliminates explanations based on impurity drag that is known to reduce the mobility of grain boundaries or interfaces in general [40]. Moreover, at a grain size of 10 nm, about 12 at% of impurities are required to form a monolayer at the grain boundaries. Although not a complete monolayer would be necessary to slow down the kinetics of boundary migration considerably, it also is unlikely that only a fraction of that value affects the kinetics drastically. The impurity effect becomes even more unlikely as a reason for the observed differences in grain boundary kinetics due to the residual equilibrium solubility in the crystalline cores of the grains and especially in the boundaries.

However, based on the results that are available so far, we can suggest that small grain sizes might be stabilized, at least kinetically, by the presence of large defect densities, especially in the region adjacent to the grain boundaries. Actually, large dislocation densities and ''rough'' grain boundaries have been observed for nanocrystalline material after severe plastic deformation [13]. If the dislocation density is very high, then the easy glide planes can get blocked, leaving the dislocations in a ''locked'' state, similar to the mechanism described as ''exhaustion plasticity'' [41]. More work in this direction is under way. However, that possibility entails exiting new options for adjusting the microscopic structure of the grain boundary regions to design the stability of nanocrystalline materials. In that sense, proper grain boundary engineering with adjustments of the structure of the boundary itself and/or the defect structure adjacent to the grain boundaries or with second-phase doping to immobilize the bound-

aries seem to offer valuable perspectives for improving the performance of nanostructured materials also under mechanical or thermo-mechanical loading conditions, thus enabling a further step with massive nanostructured materials towards the transition from laboratory into advanced applications.

Summary

Nanocrystalline composites have been successfully synthesized at room temperature by repeated cold rolling and folding of multilayered stacks of elemental foils. The massive nano-composites are characterized by uniform phase distributions and nanoscale grain sizes. It is found that alloying in general leads to a smaller grain size at similar strain if compared to pure materials. However, for achieving grain sizes in the range of only a few tens of nanometers and for increasing the thermal stability of the fine-grained microstructure at the same time, alloying with an immiscible component with a high positive heat of mixing is most effective. For such alloys, we proposed a mechanism for thermally induced grain-size refinement that is supported by the experimental results. Moreover, the thermal stability of single-phase elemental nanocrystalline material has been discussed. The experimental results suggest that the grain boundary structure and the defect structure adjacent to the grain boundaries determine the thermal stability such that very high dislocation densities reduce the grain boundary mobility. The combined results indicate that adjustment of the defect structure at the grain boundaries or strategies based on second-phase doping to immobilize the boundaries seem to offer valuable perspectives for improving the performance of nanostructured materials also under mechanical or thermo-mechanical loading conditions.

Acknowledgements One of the authors (GW) gratefully acknowledges support by the DFG. The authors thank T. Scherer for TEM sample preparation and G.P. Dinda for rolling of the Zr–Cu sample. Moreover, the authors are indebted to Prof. R. Valiev for performing the HPT experiments and to Dr. H. Sieber for performing some of the TEM analyses.

References

1. Gleiter H (1989) Prog Mater Sci 33:223
2. Gleiter H (2000) Acta Mater 48:1
3. Würschum R, Reimann K, Grub S, Kübler A, Scharwächter P, Frank W, Kruse O, Carstanjen HD, Schaefer HE (1997) Phil Mag B 74:407
4. Chattopadhyay K, Goswami R (1997) Progr Mater Sci 42:287
5. Rösner H, Weissmüller J, Wilde G (2004) Phil Mag Lett 84:673
6. Rösner H, Wilde G (2006) Scripta Mater 55:119
7. Weissmüller J, Bunzel P, Wilde G (2004) Scripta Mater 51:813
8. Wilde G (2006) Surf Interf Anal 38:1047
9. Valiev RZ, Islamgaliev RK, Alexandrov IV (2000) Prog Mater Sci 45:103
10. Valiev RZ (2002) Nature 419:887
11. Dinda GP, Rösner H, Wilde G (2005) Scripta Mater 52:577
12. Wilde G, Rösner H, Dinda GP (2005) Adv Eng Mater 7 11
13. Wilde G, Boucharat N, Dinda GP, Rösner H, Valiev RZ (2006) Mater Sci Forum 503–504: 425
14. Wilde G, Boucharat N, Hebert RJ, Rösner H, Tong S, Perepezko JH (2003) Adv Eng Mater 5:125
15. Boucharat N, Hebert RJ, Rösner H, Valiev RZ, Wilde G (2005) Scripta Mater 53:823
16. Hebert RJ, Perepezko JH, Rösner H, Wilde G (2006) Scripta Mater 54:25
17. Rösner H, Scheer P, Weissmüller J, Wilde G (2003) Phil Mag Lett 83:511
18. Johnson WL (1986) Prog Matre Sci 30: 81
19. Fecht HJ, Hellstern E, Fu Z, Johnson WL (1990) Metall Trans A 21:2333
20. Atzmon M, Veerhoeven JR, Gibson ER, Johnson WL (1984) Appl Phys Lett 45:1052
21. Bordeaux F, Yavari R (1990) Z Metallkde 81:130
22. Dinda GP, Rösner H, Wilde G (2004) In: Zhu YT, Langdon TG, Valiev RZ, Semiatin SL, Shin DH, Lowe TC (eds) Ultrafine-grained materials III. TMS, p 309
23. Dinda GP, Rösner H, Wilde G (2005) Mater Sci Eng A 410–411:328
24. Sauvage X, Wetscher F, Pareige P (2005) Acta Mater 53: 2127
25. Wilde G, Sieber H, Perepezko JH (1999) Scripta Mater 40:779
26. Butrymowicz DB, Manning JR, Read ME (1997) Diffusion Rate Data and Mass Transport Phenomena for Copper Systems. International Copper Research Association, NIST, Washington, USA, pp 193–198
27. Wilde G, Dinda GP, Rösner H, to be published
28. Weissmüller J (1993) Nanostruct Mater 3:261
29. Massalski TB (ed) (1986) Binary alloy phase diagrams, vol 1. ASM, Metals Park, OH, p 29
30. Murray JL (1984) Metall Trans A 15:261
31. Sheng HW, Wilde G, Ma E (2002) Acta Mater 50:475
32. Uenishi K, Kobayashi KF, Ishihara KY, Shingu PH (1991) Mater Sci Eng A 134:1342
33. Najafabadi R, Srolovitz DJ, Ma E, Atzmon M (1993) J Appl Phys 74:3144
34. Klassen T, Herr U, Averback RS (1997) Acta Mater 45:2921
35. Heim U, Schwitzgebel G (1999) Nanostruct Mater 12:19
36. Srdic VV, Winterer M, Hahn H (2000) J Am Ceram Soc 83:1853
37. Nakagawa Y (1958) Acta Met 6:704
38. Keblinski P, Wolf D, Phillpot SR, Gleiter H (1997) Phil Mag Lett 76:143
39. Schiotz J (2004) Mater Sci Eng A 375–377:975
40. Vilenkin A (2001) Interf Sci 9:323
41. Mishra RS, Valiev RZ, McFadden SX, Mukherjee AK (1998) Mater Sci Eng A 252:174